MAGNETIC SUSCEPTIBILITY DISACCOMMODATION AND MÖSSBAUER EFFECT IN MICROCRYSTALLINE Fe–Si RIBBONS

W.H. CIURZYŃSKA

Institute of Physics, Technical University of Częstochowa
Al. Armii Krajowej 19, 42-200 Częstochowa, Poland

(Received November 30, 1999)

In memory of Professor Jerzy Wojciech Moroń

The magnetic susceptibility disaccommodation of the microcrystalline Fe–xSi (x = 3, 5, 6.5, and 7.2 wt%) ribbons in the as-quenched state and after annealing at 1370 K for 1 h was investigated in the temperature range from 220 to 410 K. Simultaneously, the microstructure of those samples was studied using the Mössbauer spectroscopy. It is found that the isochronal disaccommodation curves may be decomposed into five elementary processes. Taking into account the results obtained from the Mössbauer spectra analysis, the relaxational process with activation energy equal to 0.84 eV may be considered as the Snoek relaxation. However, the relaxational processes of higher activation energy seem to be connected with jumps of C atoms in the vicinity of Fe atoms surrounded by 1, 2, 3, and 4 silicon atoms.

PACS numbers: 75.60.Lr, 76.80.+y

1. Introduction

Many experimental investigations have been devoted to the disaccommodation phenomenon in metals with $A2$ structure. It was found that the magnetic susceptibility disaccommodation (MSD) in these metals is connected with directional ordering of the interstitial solute atoms (i), e.g. C and N [1]. The relaxation spectrum observed in α-Fe containing C or N (e.g. [1–3]) appears in the temperature range 245–259 K due to the jumps of interstitials in the vicinity of Fe atoms (the Snoek relaxation). From investigations carried out for α-Fe–3wt%Si alloys in the form of sheets and monocrystals it was found [4–9] that the magnetic susceptibility disaccommodation band is considerably broader than in Fe–C(N) and consists of two parts:

1. the low temperature part originating from the Snoek relaxation occurring also in α-Fe–C(N) alloys,

2. the part at higher temperature originating from C and/or N atoms jumping near silicon atoms.

In the case of Fe–Si alloys containing more than 3 wt% Si, the observed relaxation spectrum is more complex [10–18]. However, the origin of that phenomenon has not been explained until now.

The aim of this paper is to find the origin of the magnetic susceptibility disaccommodation in microcrystalline Fe–xSi (x = 3, 5, 6.5, and 7.2 wt%) ribbons in the as-quenched state and after annealing at 1370 K for 1 h. In order to explain the dependence of the MSD intensity on silicon content, the microstructure of the mentioned ribbons was investigated using the Mössbauer spectroscopy.

2. Samples and experimental procedure

Microcrystalline Fe–xSi (x = 3, 5, 6.5, and 7.2 wt%) ribbons were made by rapid quenching from the melt using the single roller method. Their thickness and width were 20 μm and 10 mm, respectively. The composition of iron used for the preparation of Fe–Si samples is presented in Table I. Moreover, the purity of silicon was greater than 99.999%.

TABLE I

The impurity content in iron (wt%) used for the preparation of Fe–Si ribbons.

C	S	P	Si	Mn	Cu	O
< 0.005	< 0.005	< 0.0012	< 0.018	< 0.0016	< 0.002	< 0.097

The measurements of the susceptibility (χ) of the Fe–xSi (x = 3, 5, 6.5, and 7.2 wt%) ribbons in the as-quenched state and after annealing in vacuum at 1370 K for 1 h (pressure p = 0.5 Pa, cooling rate after heating from 1370 K to room temperature k = 360 K/min) were performed by means of a Maxwell–Wien bridge. The magnetizing field amplitude and frequency were equal to 0.16 A/m and 3.03 kHz, respectively. From the measurements of the magnetic susceptibility, the isochronal disaccommodation $\Delta(1/\chi) = 1/\chi_2 - 1/\chi_1$ versus temperature (T) was constructed: $1/\chi_2$ and $1/\chi_1$ are reciprocal magnetic susceptibilities at times t_1 = 25 s and t_2 = 295 s after demagnetization of the samples.

The $\Delta(1/\chi) = f(T)$ curves were decomposed into elementary processes, each of them being described by a single time constant. The theoretical curves were calculated using the formula [19]:

$$\Delta\left(\frac{1}{\chi}\right) = \frac{1}{\chi_2} - \frac{1}{\chi_1} = \sum_{i=1}^{n} A_i \left[\exp\left(-\frac{t_1}{\theta_i}\right) - \exp\left(-\frac{t_2}{\theta_i}\right)\right] \tag{1}$$

with

$$\theta_i = \theta_{0i} \exp\left(\frac{Q_i}{kT}\right), \tag{2}$$

where Q_i is the activation energy, θ_{0i} — pre-exponential factor and A_i — relaxation intensity of the i-th process [2, 3, 19].

The microstructure of Fe–xSi ($x = 3, 5, 6.5$, and 7.2 wt%) samples was examined using the Mössbauer spectroscopy (MS). The transmission Mössbauer spectra for the samples with the thickness of about 20 μm were measured at room temperature by means of a conventional constant acceleration spectrometer with ^{57}Co in a Rh source of 25 mCi activity. The Mössbauer spectra were analysed with a least-squares method by superimposing sets of the Zeeman sextets. The ratios of the relative line intensities in the Zeeman sextets were $A_{1,6} : A_{2,5} : A_{3,4} = 3 : A_{2,5} : 1$, where $A_{2,5}$ was fitted and assumed the same for all subspectra in each Mössbauer spectrum. From the analysis of the Mössbauer spectra, the magnetization distribution, average hyperfine field at the ^{57}Fe nuclei and order degree were also determined.

The long range order parameters (S_1 for DO_3 and S_2 for $B2$ structures) were calculated from the equations

$$S_1 = 2\left(P_A^{\beta} - P_A^{\alpha}\right) \tag{3}$$

and

$$S_2 = 2\left(P_A^{\gamma} - c_A\right), \tag{4}$$

where P_A^{β}, P_A^{α}, and P_A^{γ} are probabilities for iron atoms to occupy corresponding sites in bcc lattice (α, β are sites of Fe and Si atoms in the body and γ — in the corner of the cell) and c_A is the iron content [20].

However, the short range order parameter α_1 (the Cowley–Warren parameter) for the first coordination zone was determined from

$$\alpha_1 = 1 - \frac{P_B}{1 - c_B}, \tag{5}$$

where P_B are probabilities of the occurrence of Si atoms in the first coordination zone of the iron atom and c_B is the silicon content [21].

All studies were performed for the samples in the as-quenched state and after annealing at 1370 K for 1 h.

Additionally, the observation of the domain structure in the individual grains of annealed specimens was carried out by means of the Bitter method.

3. Results

In Fig. 1 the dependence of the magnetic susceptibility (measured at $t_1 = 25$ s after demagnetization) on the temperature, obtained for Fe–xSi ($x = 3$, 5, 6.5, and 7.2 wt%) samples after annealing at 1370 K for 1 h, is presented. The inset in Fig. 1 shows, as an example, the magnetic susceptibility of Fe–7.2%Si ribbon in the as-quenched state and after annealing at 1370 K for 1 h. As can be seen from this inset, the magnetic susceptibility of Fe–7.2%Si sample in the as-quenched state only slightly depends on the temperature. The Fe–xSi ($x = 3$, 5 and 6.5 wt%) samples in the as-quenched state exhibit the similar behaviour. Annealing of the Fe–xSi ($x = 3$, 5, 6.5, and 7.2 wt%) samples at 1370 K for 1 h leads to the increase in the magnetic susceptibility in comparison with χ of the samples in the as-quenched state; e.g. for Fe–7.2%Si sample χ at room temperature increases about 4 times (from 400 to 1780). The values of the magnetic susceptibility, obtained for the samples in the as-quenched state and after annealing at 1370 K for

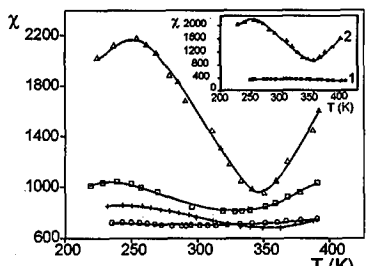

Fig. 1

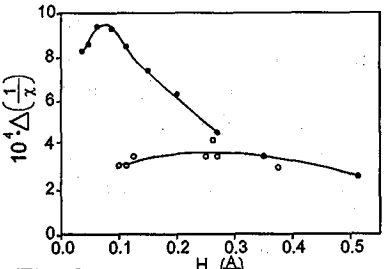

Fig. 2

Fig. 1. The dependence $\chi = f(T)$ for the Fe–xSi microcrystalline ribbons after annealing at 1370 K for 1 h: $x = 3$ (o), $x = 5$ (+), $x = 6.5$ (□) and $x = 7.2$ wt% (△). The inset: the relationship $\chi = f(T)$ obtained for the Fe–7.2%Si ribbons in as-quenched state (curve 1) and after annealing at 1370 K for 1 h (curve 2).

Fig. 2. The dependence $\Delta(1/\chi) = f(H_m)$ for the Fe–5%Si ribbons in the as-quenched state (o) and after annealing at 1370 K for 1 h (•).

TABLE II

The values of magnetic susceptibility (measured at room temperature, $t_1 = 25$ s after demagnetization) for the microcrystalline Fe–xSi ($x = 3$, 5, 6.5, and 7.2 wt%) samples in the as-quenched state (As-q) and after annealing at 1370 K for 1 h (Ann).

	Fe–3%Si		Fe–5%Si		Fe–6.5%Si		Fe–7.2%Si	
	As-q	Ann	As-q	Ann	As-q	Ann	As-q	Ann
χ	60	700	190	780	280	850	400	1780

1 h, measured at room temperature at $t_1 = 25$ s after demagnetization, are listed in Table II.

The shape of $\chi = f(T)$ curves of annealed samples (Fig. 1) depends on the silicon concentration: the higher content of Si involves the greater changes in $\chi = f(T)$ curves.

In Fig. 2 the isochronal disaccommodation $\Delta(1/\chi)$ versus the amplitude of the magnetizing field (H_m), obtained for Fe–5%Si ribbons in the as-quenched state and after annealing at 1370 K for 1 h, as an example, is presented. The disaccommodation intensity reaches a maximum at $H_m = H_s$ (stabilization field) and then monotonically decreases. As can be seen, for the annealed sample the disaccommodation intensity is higher and stabilization field is lower in comparison with the sample in the as-quenched state. Similar results were obtained for the Fe–xSi ($x = 3$, 6.5, and 7.2 wt%) samples.

In Fig. 3 the $\Delta(1/\chi) = f(T)$ curves obtained for Fe–xSi ($x = 3$, 5, 6.5, and 7.2 wt%) ribbons after annealing at 1370 K for 1 h are shown. As can be seen, the disaccommodation band occurs in the temperature region from 240 to 400 K. The shape of the $\Delta(1/\chi) = f(T)$ curves, obtained for different alloys depends on the concentration of Si atoms. For Fe–3wt%Si a high maximum occurs at 250 K.

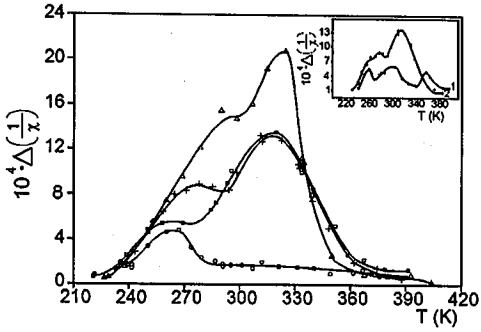

Fig. 3. The dependence $\Delta(1/\chi) = f(T)$ obtained for Fe–xSi microcrystalline ribbons after annealing at 1370 K for 1 h: $x = 3$ (o), $x = 5$ (+), $x = 6.5$ (□) and $x = 7.2$ wt% (△). The inset: the relationship $\Delta(1/\chi) = f(T)$ obtained for Fe–5%Si in the as-quenched state (curve 1) and after annealing at 1370 K for 1 h (curve 2).

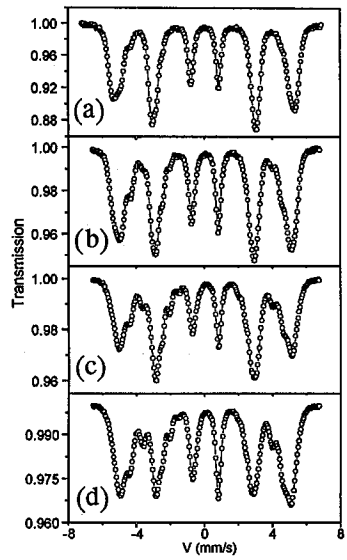

Fig. 4. Transmission Mössbauer spectra for Fe–xSi ($x = 3$, 5, 6.5, and 7.2 wt%) after annealing at 1370 K for 1 h; $x = 3$ (a), $x = 5$ (b), $x = 6.5$ (c) and $x = 7.2$ wt% (d).

For the Fe–xSi ($x = 5$, 6.5, and 7.2 wt%) samples two distinct maxima in the isochronal disaccommodation curves are observed. The inset shows, as an example, $\Delta(1/\chi) = f(T)$ curves obtained for the Fe–5%Si samples in the as-quenched state and after annealing at 1370 K for 1 h. As can be seen from the inset in this figure, the annealing of the samples causes the increase in the disaccommodation intensity.

Figure 4 shows the transmission Mössbauer spectra for the Fe–xSi ($x = 3$, 5, 6.5, and 7.2 wt%) samples after annealing at 1370 K for 1 h. As can be seen from this figure, the observed Mössbauer spectra exhibit a complex structure.

4. Discussion

The existence of migrational relaxation processes in microcrystalline Fe–Si ribbons containing C and/or N in solid solution is proved by the occurrence of the phenomenon of magnetic susceptibility disaccommodation. The form of the $\Delta(1/\chi) = f(H_m)$ curve, showing a marked maximum at $H_m = 0.9$ A/m (Fig. 2), indicates that in the studied ribbons the disaccommodation process is primarily associated with migrational relaxations in the 180° domain walls [14, 22]. Additionally, it was confirmed by the domain structure observation. It is seen (Fig. 5) that the domain patterns mainly consist of the domains separated by the 180° Bloch walls.

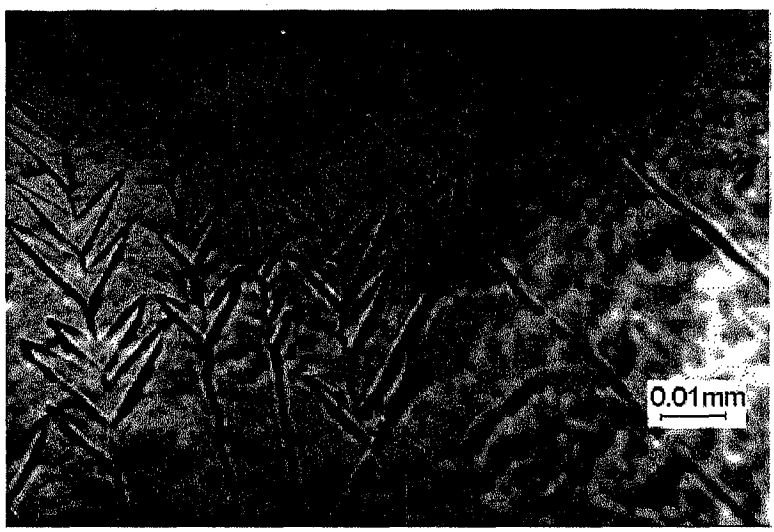

Fig. 5. The domain structure in the Fe–6.5%Si microcrystalline samples annealed at 1370 K for 1 h.

The band of the disaccommodation in investigated microcrystalline Fe–xSi ($x = 3$, 5, 6.5, and 7.2 wt%) alloys occurs in the temperature region from 240 to 400 K, i.e. within a similar temperature range as in the case of Fe–Si monocrystals and transformer sheets (e.g. [7]). The experimental $\Delta(1/\chi) = f(T)$ curves were decomposed into five elementary processes of single time constants θ_i. Figure 6 shows, as an example, the decomposition of the $\Delta(1/\chi) = f(T)$ curve obtained for the Fe–5wt%Si ribbon annealed at 1370 K for 1 h; the broken lines are the particular elementary processes and the solid line is the sum of them.

In Table III the activation energy (Q_i) and intensity of elementary processes (A_i) are listed. θ_{0i} was imposed to be 3.2×10^{-15} s, according to [2, 3]. The process with the activation energy equal to 0.84 eV corresponds to the carbon Snoek relaxation in Fe [2, 3]. Taking into account the contribution of elementary processes (I, II, III, IV, and V) to the MSD phenomenon, one can see (Fig. 7) that the $A_I/\sum A_i$ and $A_{II}/\sum A_i$ ratios decrease and $A_{III}/\sum A_i$, $A_{IV}/\sum A_i$ and $A_V/\sum A_i$ (where $i = 1, 2, 3, 4, 5$) increase with Si content faster than linearly.

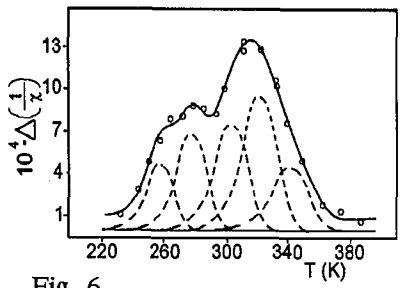

Fig. 6

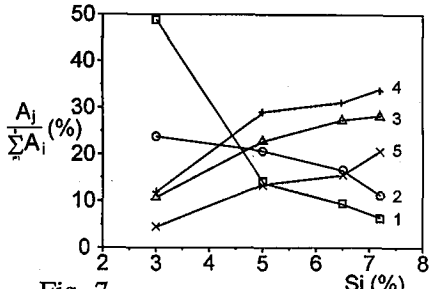

Fig. 7

Fig. 6. Results of the $\Delta(1/\chi) = f(T)$ curve analysis obtained for the Fe–5%Si ribbons after annealing at 1370 K for 1 h: (o) experimental data, (- - -) theoretical curves of elementary processes; (—) sum of theoretical curves.

Fig. 7. The dependence $A_j/\left(\sum_{i=1}^{5} A_i\right)$ versus Si concentration for elementary processes I–V (curves 1–5, respectively).

TABLE III

Activation energies (Q [eV]) and intensities (A [$\times 10^{-4}$]) of the elementary processes obtained for the microcrystalline Fe–xSi (x = 3, 5, 6.5, and 7.2 wt%) ribbons after annealing at 1370 K for 1 h.

Sample	Peak I		Peak II		Peak III		Peak IV		Peak V	
	Q	A	Q	A	Q	A	Q	A	Q	A
Fe–3%Si	0.84	8.6	0.90	4.2	0.98	1.9	1.07	2.1	1.18	0.8
Fe–5%Si	0.84	6.4	0.91	9.4	0.99	10.4	1.05	13.2	1.12	6.1
Fe–6.5%Si	0.85	4.9	0.92	8.6	0.97	16.0	1.03	13.9	1.11	8.0
Fe–7.2%Si	0.84	3.8	0.88	6.8	0.94	17.1	1.03	20.5	1.08	12.6

From analysis of the Mössbauer spectra it was found that the probabilities (equal to the relative areas of the corresponding sextets) for iron atoms to have 8, 7, 6, 5, and 4 Fe atoms as the nearest neighbours (nn) depend on the silicon concentration (Fig. 8 and Table IV). The probability of the occurrence of 8 and 7 Fe atoms as nearest neighbours of ^{57}Fe nuclei decreases and 6, 5 and 4 increases with increasing Si content in the samples (Fig. 8).

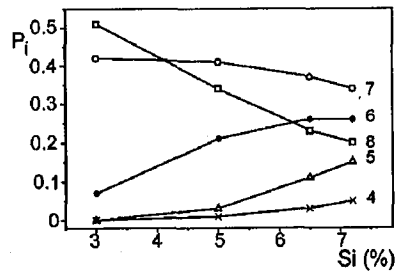

Fig. 8. The probability of the occurrence of 8, 7, 6, 5, and 4 Fe atoms as nearest neighbours of ^{57}Fe nuclei (curves 8, 7, 6, 5, and 4, respectively).

TABLE IV

The probabilities for iron atom to have 8, 7, 6, 5, 4 iron atoms as nearest neighbours (P_8, P_7, P_6, P_5, P_4) obtained for binomial distribution (Bin) and data from the Mössbauer spectra analysis for the microcrystalline Fe–xSi (x = 3, 5, 6.5, and 7.2 wt%) samples in the as-quenched state (As-q) and after annealing at 1370 K for 1 h (Ann), long and short range order parameters (S_1 for DO_3, S_2 for $B2$ and α_s obtained from Eqs. (3)–(5)) and the second line intensity in the Zeeman sextets ($A_{2,5}$).

	Fe–3%Si			Fe–5%Si			Fe–6.5%Si			Fe–7.2%Si		
	Bin	As-q	Ann	Bin	As-q	Ann	Bin	As-q	Ann	Bin	As-q	Ann
P_8	0.58	0.52	0.51	0.45	0.37	0.34	0.36	0.28	0.23	0.32	0.21	0.20
P_7	0.33	0.42	0.42	0.38	0.42	0.41	0.39	0.37	0.37	0.39	0.36	0.34
P_6	0.08	0.06	0.07	0.14	0.19	0.21	0.19	0.26	0.26	0.21	0.28	0.26
P_5	0.01			0.03	0.02	0.03	0.05	0.08	0.11	0.07	0.14	0.15
P_4						0.01	0.01	0.01	0.03	0.01	0.03	0.05
$A_{2,5}$		2.3	2.8		2.1	2.4		2.2	2.8		1.8	2.5
					1.62							
S_1		1.29	1.06		($Fe_{15}Si$)							
		($Fe_{15}Si$)			1.6							
					(Fe_7Si)							
S_2		0.27	0.27		0.38							0.53
α						−0.4		-0.25	−0.4		−0.35	−0.8

One may conclude (from Figs. 7 and 8) that a close relation between the configuration of iron atoms in bcc lattice and the intensities of elementary relaxation processes (I, II, III, IV, and V) exists. The increase in the probability for iron atom to have 6, 5, and 4 Fe atoms as nn corresponds to the increase in the intensity of elementary processes III, IV, and V responsible for the observed magnetic susceptibility disaccommodation. Simultaneously, the decrease in the probability of the occurrence of 8 and 7 Fe atoms as nn of ^{57}Fe nuclei takes place which corresponds to the decrease in the intensity of the I and II elementary relaxational processes (Table III, Fig. 7). Thus, the relaxation elementary processes III, IV, and V may be connected with jumping of C atoms in the neighbourhood of Fe atoms having 6, 5, and 4 Fe atoms (i.e. 2, 3, and 4 Si atoms) as nearest neighbours. However, the elementary process II (Fig. 7, Table III) may be caused by migration of C atoms in the vicinity of Fe atoms having 7 Fe atoms (i.e. one Si atom) as nearest neighbours.

It is worth noting that silicon atoms are not randomly distributed in α-Fe–Si lattice because the results obtained from the Mössbauer spectra analysis (Table IV) differ from those obtained for binomial distribution. The Mössbauer spectrum for Fe–3%Si is decomposed into three Zeeman sextets corresponding to ^{57}Fe atoms having 8, 7, and 6 Fe atoms as nearest neighbours. The ratios of intensities of these Zeeman sextets indicate that $B2$ and $Fe_{15}Si$ superstructure occurs in both as-quenched and annealed samples with S_1 and S_2 order parameters listed in Table IV. Similar results are obtained for the as-quenched Fe–5%Si sample where

$B2$ and $Fe_{15}Si$ and Fe_7Si types of superstructure appear. Annealing that sample at 1370 K for 1 h and subsequent fast cooling to room temperature changes the long range order into short range order with the parameter $\alpha = -0.4$. For the Fe–6.5%Si and Fe–7.2%Si alloy the parameter of the short range order increases after annealing the samples. Additionally, $B2$ superstructure appears after the annealing of the Fe–7.2%Si samples.

From the Mössbauer spectra analysis it was also found (Table IV) that the magnetization vector in the as-quenched samples is almost randomly distributed. This is caused by the internal stresses that originate from defects introduced during the ribbon preparation. These internal stresses act as pinning centres for domain walls and strongly influence the magnetic properties in the as-quenched state, i.e. involve the low value of the initial susceptibility (the inset in Fig. 1). These structural defects influence also the intensity of the magnetic susceptibility disaccommodation (the inset in Fig. 3) because some of relaxators are blocked in the strain field of defects [23]. The magnetization vector in annealed ribbons exhibits a tendency to align parallel to the sample surface (Table IV) because of the stress relief of the samples. That relieving leads to the increase in both the magnetic susceptibility and intensity of disaccommodation.

Summing up the results obtained in this paper, the MSD band in microcrystalline Fe–xSi (x = 3, 5, 6.5, and 7.2 wt%) ribbons originates from five elementary processes: the carbon Snoek relaxation (directional ordering of single carbon atoms in octahedral sites surrounded by Fe atoms) and relaxations originating from jumps of C atoms in the vicinity of Fe atoms surrounded by 7, 6, 5, and 4 Fe atoms (i.e. one, two, three, and four Si atoms).

It is worth noting that the annealing of the Fe–xSi (x = 3, 5, 6.5, and 7.2 wt%) samples at 1370 K for 1 h not only causes the increase in magnetic susceptibility in comparison with χ for the as-quenched samples but changes the shape of the $\chi = f(T)$ curves as well. The character of these curves depends on the concentration of Si atoms: the higher concentration of Si atoms the greater changes of the $\chi = f(T)$ shape.

5. Conclusions

1. Magnetic susceptibility disaccommodation in microcrystalline Fe–xSi (x = 3, 5, 6.5, and 7.2 wt%) ribbons is mainly connected with migrational processes in 180° Bloch walls.

2. The isochronal disaccommodation curves may be decomposed into five elementary processes (I–V).

3. The correlation between the microstructure and intensity of the magnetic susceptibility disaccommodation is found. The elementary relaxational processes I–V are connected with jumping of C atoms in neighbourhood of Fe atoms having 8 iron atoms (the Snoek relaxation — process I), and 7, 6, 5 and 4 Fe atoms (i.e. 1, 2, 3 and 4 Si atoms) as nearest neighbours (processes II–V).

Acknowledgments

The paper was financially supported by the Committee for Scientific Research (grant No. 7 T082 022 17).

References

[1] H. Kronmüller, *Nachwirkung in Ferromagnetika*, Springer, Berlin 1968.

[2] L. Kozłowski, J.W. Moroń, J. Przybyła, J. Rasek, *Acta Phys. Pol. A* **40**, 445 (1971).

[3] L. Kozłowski, J.W. Moroń, J. Rasek, *Phys. Status Solidi A* **13**, 601 (1972).

[4] A. Ferro, G. Montalenti, *Ricerca Scientifica* **25**, 3069 (1955).

[5] H. Fahlenbrach, E. Houdremont, *Archiv. Eisenhüttenw.* **25**, 377 (1954).

[6] M. Markuszewicz, B. Wysłocki, K. Stoiński, *Acta Phys. Pol. A* **23**, 59 (1963).

[7] J.W. Moroń, *Acta Phys. Pol. A* **26**, 1117 (1964).

[8] K. Tsushima, M. Asanama, S. Miyahara, *J. Phys. Soc. Japan* **14**, 1233 (1959).

[9] K. Tsushima, *J. Phys. Soc. Japan, Suppl. BI* **17**, 338 (1962).

[10] J. Bosman, P.E. Brommer, G.W. Rathenau, *J. Phys. Rad. (France)* **20**, 241 (1959).

[11] W. Ciurzyńska, J.W. Moroń, B. Wysłocki, Y. Yamashiro, *Acta Phys. Pol. A* **68**, 523 (1985).

[12] W. Ciurzyńska, Y. Yamashiro, J.W. Moroń, J. Zbroszczyk, B. Wysłocki, *Acta Phys. Pol. A* **72**, 141 (1987).

[13] W. Ciurzyńska, B. Wysłocki, J.W. Moroń, Y. Yamashiro, J. Zbroszczyk, *Physica B* **146**, 416 (1987).

[14] W. Ciurzyńska, B. Wysłocki, J.W. Moroń, Y. Yamashiro, in: *Conf. Proc. Soft Magnetic Materials 7, Blackpool 1985*, Ed. J.E. Thompson, Wolfson Centre for Magnetics Technology, Cardiff 1985, p. 118.

[15] W. Ciurzyńska, J. Zbroszczyk, J. Olszewski, J. Frąckowiak, K. Narita, *J. Magn. Magn. Mater.* **133**, 351 (1994).

[16] W. Ciurzyńska, J. Zbroszczyk, J. Olszewski, J. Frąckowiak, J. Świerczek, B. Wysłocki, S. Szymura, *J. Magn. Magn. Mater.* **140-144**, 87 (1995).

[17] W. Ciurzyńska, J.W. Moroń, J. Zbroszczyk, B. Wysłocki, S. Szymura, J. Rasek, Y. Yamashiro, *Mater. Sci. Forum* **119-121**, 95 (1993).

[18] W. Ciurzyńska, *J. Magn. Magn. Mater.* **140-144**, 87 (1998).

[19] J. Rasek, *Acta Phys. Pol. A* **44**, 85 (1973).

[20] P.S. Rudman, *Acta Metall.* **8**, 321 (1960).

[21] J.M. Cowley, *Phys. Rev.* **120**, 1648 (1960).

[22] L. Néel, *J. Phys. Rad. (France)* **13**, 249 (1952).

[23] F. Walz, H.J. Blythe, W. Merz, *Acta Metall.* **31**, 145 (1983).